Catalysis Today 178 (2011) 103–109

Contents lists available at SciVerse ScienceDirect

Catalysis Today

journal homepage: www.elsevier.com/locate/cattod

Kinetics of formation of chromia promoted skeletal iron catalysts for the water gas shift reaction

Thomas M. Leoni*, Mark S. Wainwright

ARC Center of Excellence for Functional Nanomaterials, School of Chemical Engineering, University of New South Wales, Sydney, NSW 2052, Australia

ARTICLE INFO

Article history:
Received 21 June 2011
Received in revised form 8 August 2011
Accepted 14 August 2011
Available online 9 September 2011

Keywords:
Skeletal iron
Water–gas-shift
Leaching kinetics
Iron catalyst
Chromium promotion
Fe_2Al_5

ABSTRACT

Particles of Fe_2Al_5 (60–211 μm diameter) were leached at 10, 30 and 50 °C in 3 M NaOH containing varying amounts of sodium chromate in the range 0.005–0.05 M. The kinetics of leaching was fitted to solid-state kinetic models. The model best fitting the data was the Avrami–Erofeev model $-\ln(1-\alpha)^{1/1.5} = kt$. Apparent activation energies were in the range 60–63 kJ mol^{-1}. The BET surface areas of the promoted materials were high, with values in the range 57–91 m^2 g^{-1}. Catalysts were tested for the water–gas-shift (WGS) reaction at 350 °C and it was found that the chromium content of the catalysts had a significant effect on the WGS activity, which went through a maximum for a catalyst containing around 2 wt% chromium.

1. Introduction

Skeletal catalysts have been used for nearly a century since Murray Raney's discovery of a spongy, active form of nickel obtained by leaching nickel/silicon or nickel/aluminium alloys in concentrated caustic solutions [1–4]. Systems based on other transition metals such as Au, Ag, Cu, Co, Fe, Ti and Ru alloyed with Al have been studied, with numerous studies of Raney® Ni, Cu and Co catalysts which are available commercially and widely used in industry. Paul and Hilly [5] were the first to study skeletal Fe formed by caustic leaching of a 20 wt% Fe/80 wt% Al alloy. More recently, Leoni [6] has made a comprehensive study of a large range of skeletal Fe catalysts produced from Fe–Al alloys with a wide range of compositions.

Porous iron catalysts are used in two important energy processes, the Fischer–Tropsch synthesis and the high-temperature water–gas-shift reaction [7]. There have been a number of studies of skeletal iron for the Fischer–Tropsch process [8–11]. However, there have been no studies of chromium promotion of skeletal iron or its use in the WGS reaction. There have been several major reviews of the WGS reaction [12–15], however, the iron–chromium catalysts are produced by either a precipitation route using iron and chromium salts or through impregnation of Fe_2O_3 with a chromate solution. This paper describes the leaching kinetics of Fe_2Al_5 in 3 M aqueous NaOH with different concentrations of Na_2CrO_4. The catalytic properties of the chromia promoted skeletal iron formed, including a preliminary investigation of activity for the WGS reaction, are also reported.

2. Materials and methods

2.1. Leaching kinetics and catalyst characterisation

It has been shown by Leoni and co-workers [16] that the iron aluminide Fe_2Al_5 (comprised of 54.2 wt% Al and 45.8 wt% Fe) produces high BET surface area skeletal iron when small particles (150–211 μm) are leached at 10 °C in 3 M aqueous NaOH. The effect of chromate addition on the kinetics of leaching of Fe_2Al_5 particles in the range of 60–211 μm was studied by adding different concentrations of sodium chromate in the range 0.005–0.05 M in 3 M NaOH solutions. Upon dissolution in an ultrasonic bath, clear, yellow leaching solutions were obtained and stored in sealable polyethylene containers. Leaching experiments were conducted in a four-neck glass vessel, fitted with a valve for the introduction of Fe_2Al_5 alloy particles, a septum with a line to the MilliGasCounter wet gas meter, an Inconel600 thermocouple for measuring the temperature and a port for the introduction of the leaching solution. Accurate temperature control to ±0.1 °C was provided using a Haake Fisons k20 thermostat with a DC3 circulator. A stirrer was not fitted to the experimental setup, since it was shown that stirring had no effect on the kinetics of the leaching reaction [16]. In a typical leaching experiment, 1.0 g of alloy was leached in 100 ml 3 M NaOH containing sodium chromate, with the OH^-/Al ratio in excess

* Corresponding author. Tel.: +61 293857994.
E-mail addresses: t.leoni@unsw.edu.au (T.M. Leoni), mark.wainwright@unsw.edu.au (M.S. Wainwright).

0920-5861/$ – see front matter © 2011 Elsevier B.V. All rights reserved.
doi:10.1016/j.cattod.2011.08.027

of 14.5:1. The reaction was carried out until the wet gas meter stopped recording any hydrogen evolution. The leached material was then removed using a 60 ml polyethylene syringe and collected with a strong magnet before being gently flushed into a polyethylene container. All leached materials were subsequently washed with H_2O, which was treated through a MilliQ station, until the water was clear and pH reached 7. Subsequently, the moist product was washed five times with dry pyridine and then stored under dry pyridine until further analyses, including compositions and BET surface areas, were made.

BET and pore size distribution measurements were obtained using nitrogen adsorption/desorption measurements on a Micromeritics Tristar 3000 system. Alloy composition was determined on acid-digested samples using inductively coupled plasma optical emission spectroscopy (ICP-OES). A Philips X'pert Multipurpose X-ray Diffraction System was used to record the XRD patterns for both the alloy and the leached materials. Scanning electron microscope images were taken with a Hitachi S900 and energy dispersive X-ray maps of the leached materials were recorded using a Hitachi S3400, which was fitted with a Bruker XFlash 5010 Silicon Drift Detector. The chemical compositions of the leached materials were measured using a Philips PW2400 Sequential X-Ray Fluorescence Spectrometer.

2.2. Catalyst activity for the water–gas-shift reaction

Additional catalyst samples were prepared to test the activity of unpromoted and chromia promoted skeletal iron for the water-gas-shift reaction;

$$CO + H_2O \leftrightarrow CO_2 + H_2 \quad (1)$$

Catalyst testing was conducted in a stainless steel tubular reactor (6 mm O.D.), which was inserted in an electric furnace and was fitted with a thermocouple to measure the temperature in the catalysis bed. Stoichiometric amounts of CO and water were used in all experiments. CO and Ar flows were set at 50 ml/min. Water was added into the gas stream using an ISCO high precision hydraulic pump (ISCO Inst., model 260D) at a rate of 37 μl/min, which was vapourised in a preheater at 200 °C. Catalyst samples were loaded in moist condition into the reactor and were retained by a quartz glass wool plug. Prior to the reactant gas stream flowing over the catalysts, the catalysts were dried in argon at 100 ml/min at 150 °C for 9 h. During the first hour of heating the bed temperature was raised from room temperature to 150 °C. Subsequently, the dried catalysts were cooled to room temperature and the reactor was re-weighed to calculate the amount of catalyst loaded. The reactor was then reinstalled in the WGS rig and the furnace bed temperature was raised to 350 °C in 2.5 h and kept at this temperature during the WGS experiment.

Prior to analysis of the product stream, it was passed over a cartridge containing fresh silica gel for water removal. The product stream was fed to two gas chromatographs (Shimadzu GC8A), which were fitted with thermal conductivity detectors. One chromatograph was operated with helium as carrier gas using a 1.8-m CTR I column (Alltech Associates, Inc) for CO and CO_2 analyses, while the second chromatograph used argon as carrier gas and a 2-m molecular sieve 13X column (Alltech Associates, Inc.) for H_2 analysis. The catalyst activity was determined by measuring the amount of carbon monoxide consumed and expressed as mmol of CO per hour per gram of catalyst.

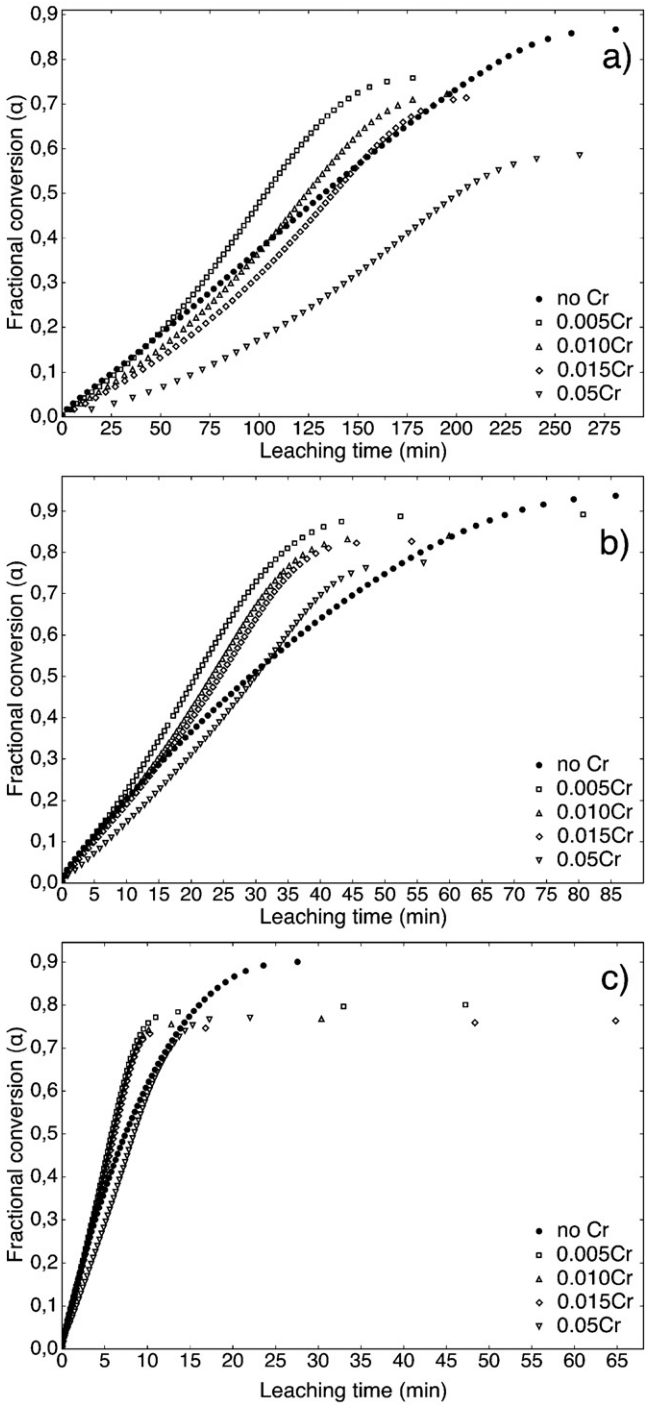

Fig. 1. Effect of Na_2CrO_4 addition on leaching curves of Fe_2Al_5 at temperatures of 10 °C (a), 30 °C (b) and 50 °C (c). Leaching conditions: 1.0 g Fe_2Al_5 (63–211 μm), 100 ml 3 M NaOH.

3. Results and discussion

3.1. Leaching kinetics modelling

The addition of chromate to the caustic has a significant effect on the kinetics of leaching compared with the kinetics without chromate [16]. Similar findings were made by Ma et al. [17] and Smith et al. [18], who studied chromium promoted skeletal copper and chromium promoted skeletal cobalt formation respectively. For both the skeletal copper and cobalt the rates for the leaching reaction decreased with increasing sodium chromate content in the

Table 1
Reaction rate constants and apparent activation energies for the best-fitting kinetic model $-\ln(1-\alpha)^{1/1.5} = kt$ of promoted and unpromoted skeletal iron.

$[Na_2CrO_4]$ (mol l^{-1})	Temperature						E_a (kJ mol^{-1})
	10 °C		30 °C		50 °C		
	k (min$^{-1} \times 10^3$)	r^2	k (min$^{-1} \times 10^3$)	r^2	k (min$^{-1} \times 10^3$)	r^2	
–	6.0	1.00	25.7	0.99	95.2	0.98	53 ± 0.1
0.005	7.7	1.00	39.2	1.00	134.3	1.00	55 ± 0.7
0.010	6.4	1.00	35.4	1.00	131.7	1.00	58 ± 0.7
0.015	5.7	1.00	24.3	0.98	130.3	1.00	59 ± 1.5
0.05	3.7	1.00	26.9	1.00	89.0	0.99	61 ± 2.0

Table 2
Initial leaching rate constants and apparent activation energies for unpromoted and promoted skeletal iron.

$[Na_2CrO_4]$ (mol l^{-1})	Temperature						E_a (kJ mol^{-1})
	10 °C		30 °C		50 °C		
	k (min$^{-1} \times 10^3$)	r^2	k (min$^{-1} \times 10^3$)	r^2	k (min$^{-1} \times 10^3$)	r^2	
–	3.8	1.00	21.9	0.99	88.0	1.00	60 ± 0.5
0.005	3.7	1.00	22.9	1.00	86.7	1.00	60 ± 1.0
0.010	3.1	1.00	20.8	1.00	86.4	1.00	63 ± 0.9
0.015	2.7	1.00	19.5	1.00	74.7	0.97	63 ± 1.4
0.05	1.6	0.99	14.6	1.00	58.5	1.00	63 ± 1.4

Table 3
Properties of unpromoted and chromium promoted skeletal iron with different Na_2CrO_4 concentrations.

$[Na_2CrO_4]$ (mol l^{-1})	Leaching temperature (°C)	α_{XRF}	S_{BET} (m^2 g^{-1})	S_{BET} normalised (m^2 g^{-1})	Pore volume, V_p (cm^3 g^{-1})	Pore diameter, d_p (nm)
–	10	0.87	70.7 ± 0.4	81.5 ± 0.5	0.155	7.5
–	30	0.94	68.2 ± 0.3	72.7 ± 0.3	0.176	8.8
–	50	0.90	57.4 ± 0.5	63.7 ± 0.6	0.190	11.6
0.005	10	0.76	78.0 ± 0.3	102.8 ± 0.4	0.092	4.4
0.005	30	0.89	77.8 ± 0.3	87.2 ± 0.3	0.109	5.4
0.005	50	0.80	82.5 ± 0.5	103.0 ± 0.6	0.145	6.6
0.010	10	0.72	56.5 ± 0.3	78.1 ± 0.4	0.063	4.2
0.010	30	0.84	79.9 ± 0.3	95.0 ± 0.4	0.105	4.8
0.010	50	0.77	74.3 ± 0.4	96.8 ± 0.5	0.117	6.0
0.015	10	0.71	72.6 ± 0.3	101.6 ± 0.4	0.084	4.5
0.015	30	0.83	90.8 ± 0.4	109.8 ± 0.5	0.117	5.0
0.015	50	0.76	85.4 ± 0.4	111.9 ± 0.5	0.123	5.6
0.05	10	0.59	73.1 ± 0.3	124.9 ± 0.5	0.079	4.0
0.05	30	0.76	84.4 ± 0.4	108.9 ± 0.5	0.097	4.5
0.05	50	0.77	77.7 ± 0.4	101.0 ± 0.5	0.118	5.5

Table 4
Compositional analysis of unpromoted and chromium promoted skeletal iron using XRF and EDX techniques.

$[Na_2CrO_4]$ (mol l^{-1})	T (°C)	α_{H_2}	α_{XRF}	XRF composition			EDX composition		
				Fe (wt%)	Al (wt%)	Cr (wt%)	Fe (wt%)	Al (wt%)	Cr (wt%)
–	10	0.88	0.87	85.1	13.0	–	70.5	2.06	–
–	30	0.93	0.94	90.5	7.7	–	81.5	2.08	–
–	50	0.95	0.90	92.2	5.9	–	76.6	1.43	–
0.005	10	0.71	0.76	71.2	25.4	1.82	64.5	2.50	2.64
0.005	30	0.84	0.89	79.6	16.0	2.05	73.3	3.12	3.05
0.005	50	0.87	0.80	81.7	13.7	2.24	69.8	1.81	4.24
0.010	10	0.62	0.72	65.7	31.0	1.77	66.6	2.45	2.88
0.010	30	0.80	0.84	75.7	19.1	2.41	72.6	2.15	3.02
0.010	50	0.84	0.77	79.3	15.3	2.71	67.5	2.72	3.82
0.015	10	0.64	0.71	65.7	29.6	1.97	65.6	2.69	2.44
0.015	30	0.77	0.83	73.8	20.7	2.57	64.1	2.01	2.71
0.015	50	0.83	0.76	78.2	16.5	3.14	66.9	2.16	3.86
0.05	10	0.66	0.59	67.8	28.3	1.97	63.5	2.54	2.24
0.05	30	0.76	0.76	73.2	22.2	2.71	69.2	2.36	3.07
0.05	50	0.79	0.77	74.9	19.8	3.10	68.5	1.54	2.99

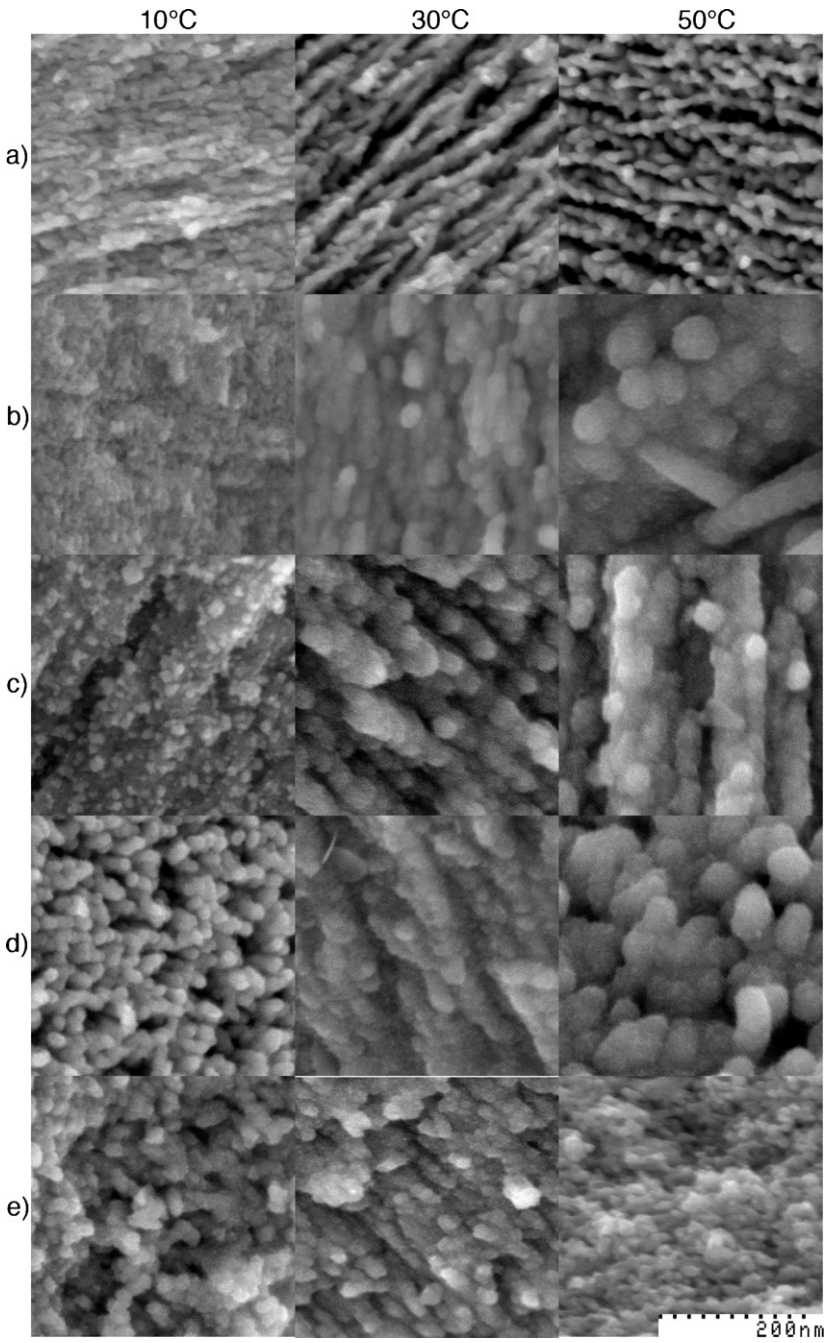

Fig. 2. Nanostructures for skeletal iron (a) without chromate, (b). 0.005 M chromate, (c) 0.010 M chromate, (d) 0.015 M chromate and (e) 0.05 M.

caustic solution. Our findings for chromium promoted skeletal iron follow the same trend (Fig. 1).

The leaching curves in Fig. 1 were fitted to a wide range of kinetic models as has been reported previously for the leaching of Fe_2Al_5 in pure NaOH solutions [16]. Table 1 summarises the kinetic rates and the apparent activation energies for the best fitting model, which was found to be the Avrami–Erofeev model

$$-\ln(1-\alpha)^{1/1.5} = kt \quad (2)$$

With increasing chromate concentration in the caustic, the kinetic rates decreased at all temperatures, while the apparent activation energies slightly increased. For chromium promoted skeletal copper [17] and cobalt [19] the same trends were observed. The higher the amount of chromate, the more pronounced was the sigmoidal shape of the leaching curves.

Initial leaching rates were calculated using the relationship given by Eq. (3)

$$\alpha = kt \quad (3)$$

for conversions up to $\alpha = 0.2$. Table 2 presents initial leaching rates and apparent activation energies. For all leaching temperatures, the values for the initial leaching rates (Table 2) show that at higher chromate concentrations the initial rates decreased, which is confirmed by the leaching curves in Fig. 1.

3.2. BET surface areas

Chromate addition not only has an effect on the kinetics of leaching, the leached products also have significantly different surface areas, as shown in Table 3. Ma and co-workers [20] found similar

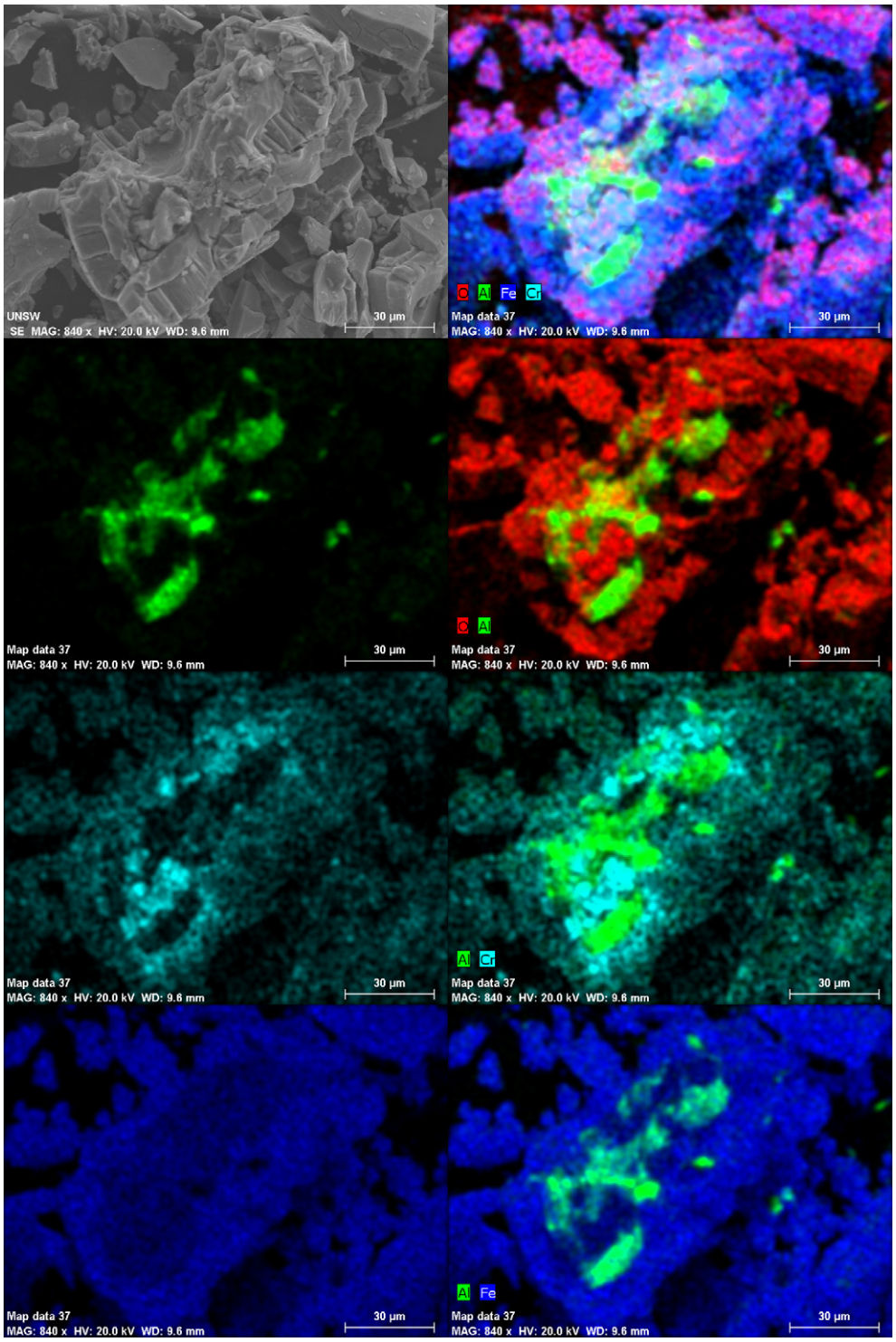

Fig. 3. Example of a core/shell structure of a Fe_2Al_5 particle, leached in 3 M. NaOH containing 0.05 M Na_2CrO_4 at 50 °C (green, Al; cyan, Cr; blue, Fe; red, O). (For interpretation of the references to color in this figure legend, the reader is referred to the web version of the article.)

effects for chromium promoted skeletal copper, as did Smith et al. [19], for chromium promoted skeletal cobalt. Table 3 shows that at the lowest concentration of chromate (0.005 M), the BET surface area increased with increasing temperature. This is indeed surprising, since when the reaction was carried out without chromate, the BET surface area decreased with increasing temperature. However, when the amount of chromate was doubled to 0.010 M, or increased further, the BET surface area showed different behaviour. For Fe_2Al_5 leached with 0.010 M, 0.015 M and 0.05 M chromate present in the 3 M NaOH, the highest values were obtained with 30 °C. Ma et al. [20] found that when $CuAl_2$ is leached at 0 °C in 6.1 M NaOH and the sodium chromate content was increased that with increasing chromium content in the catalyst the specific surface area could be tripled in value compared with unpromoted skeletal copper. Smith et al.'s study [19] found that an increasing concentration of sodium chromate produced skeletal cobalt with increased surface area, par-

Table 5
Compositional analysis of unpromoted and chromium promoted skeletal iron using XRD and EDX techniques.

$[Na_2CrO_4]$ (mol l^{-1})	T (°C)	XRF composition Cr_2O_3 (wt%)	EDX composition Cr_2O_3 (wt%)
–	10	0.01	–
–	30	0.00	–
–	50	0.00	–
0.005	10	2.66	3.86
0.005	30	3.00	4.46
0.005	50	3.28	6.20
0.010	10	2.58	4.21
0.010	30	3.52	4.41
0.010	50	3.96	5.58
0.015	10	2.88	3.57
0.015	30	3.75	3.96
0.015	50	4.59	5.64
0.05	10	2.89	3.27
0.05	30	3.96	4.49
0.05	50	4.53	4.37

ticularly over the range of 0–0.025 M sodium chromate, for which the BET areas for skeletal cobalt increased from 60 m^2 g^{-1} for the unpromoted catalyst to 100 m^2 g^{-1}.

Since the Fe_2Al_5 particles did not leach to completion, i.e. the fractional conversion was below 1, the BET specific surface areas were normalised using Eq. (4)

$$\text{Normalised } S_{BET} = \text{ Measured } S_{BET}/\alpha \quad (4)$$

where α is the fractional conversion value obtained from the hydrogen evolution curve when the experiment was terminated due to no more H_2 being evolved (Table 3). Normalisation provides a value for surface area per unit gram of converted alloy, rather than per unit gram of total alloy, which helps in understanding the true surface area achieved within the porous sections of the alloy.

Interestingly, the pore volumes of samples produced using sodium chromate in the leach liquor are smaller than for those leached in pure caustic. For skeletal copper, pore volumes also decreased with increasing chromate content [20], but not as pronounced as observed for skeletal iron, while pore volumes for skeletal cobalt went through a minimum [19]. Table 3 shows that the pore volumes increase with increasing leaching temperature for each experimental condition. Pore diameters also increase with increasing leaching temperature; however, they are quite small compared with samples leached in pure caustic solution.

3.3. Scanning electron microscopy images

The nanostructures of the chromium promoted skeletal iron catalysts are different to those of the unpromoted samples. Leaching of Fe_2Al_5 in pure 3 M NaOH leads to an organised layout of iron-rods (Fig. 2a), however when chromate is present interesting changes are observed. With 0.005 M chromate in the caustic at 10 °C (Fig. 2), the structure of the catalyst resembles that for the unpromoted one, however the scale of features is much finer. When leached at higher temperatures, the structure changes and the crystallites become bigger in size. This observation is true for all skeletal iron catalysts promoted with 0.005, 0.010 and 0.015 M sodium chromate. When the chromate concentration is further increased to 0.05 M, there is no increase in crystallite size. However, the micrographs in Fig. 2 show that the bigger crystallites are made from very small clusters, which results in smaller pores.

3.4. X-ray fluorescence and energy dispersive X-ray results

Two different techniques were used to characterise the leached materials containing chromate. Table 4 summarises the composition for the elements Fe, Al and Cr, as well as their oxides, measured by XRF and EDX. Furthermore, the EDX analysis only measures the composition on the surface of the particles, hence the major difference of the aluminium values compared to the XRF techniques since the Al is concentrated in the inner part of the particles. However, when trends of each technique are compared, they are consistent for both characterisation methods (with the exception of Al for the EDX measurements). The iron powder used to produce the Fe_2Al_5 intermetallic showed only a minor trace of chromium of 44.3 ppm. The X-ray spectra obtained by EDX did not show any chromium peak for the Fe_2Al_5 alloy or the unpromoted samples. The final fractional conversion can be calculated from XRF results using Eq. (5)

$$\alpha = 1 - \left[\frac{\text{wt\% Al}_{\text{Catalyst}}}{\text{wt\% Al}_{\text{Alloy}}} \cdot \frac{\text{wt\% Fe}_{\text{Alloy}}}{\text{wt\% Fe}_{\text{Catalyst}}}\right] \quad (5)$$

The calculated final fractional conversions from the hydrogen evolution (α_{H_2}) and XRF measurements (α_{XRF}) shown in Table 4 are in good agreement.

Of particular interest is that all samples leached in chromium promoted caustic contain a substantial amount of aluminium, as confirmed by XRF. This is consistent with the leaching curves for the chromate promotion experiments in Fig. 1, which show that the maximum fractional conversion was less than 90%. Moreover, it seems that the maximum of chromium, which can be incorporated in the skeletal iron is around 1.8–3.1 wt% (Table 4). This equates to a chromia content of around 2.5–4 wt% (Table 5). It has been observed that skeletal copper produced by leaching $CuAl_2$ in 6.1 M NaOH containing sodium chromate concentrations of 0.01 and 0.1 M led to chromia contents of 1.6–3.1 wt% [21]. EDX elemental mapping of Fe_2Al_5 particles, which were exposed to sodium chromate containing caustic, showed that the deposited chromium is distributed throughout the skeletal structure, but also show that there is a concentration of chromium around the unleached alloy core (Fig. 3). This suggests that the chromium is concentrated near the reaction front during the leaching process.

3.5. X-ray diffraction measurements

XRD patterns for all catalysts can be found in Leoni's thesis [6]. Compared with Fe_2Al_5 leached in 3 M NaOH, the leached materials

Table 6
Characteristics of chromia promoted skeletal iron catalysts used in WGS reaction.

$[Na_2CrO_4]$ (mol l^{-1})	T (°C)	XRF composition						S_{BET} (m^2 g^{-1})	α_{XRF}	S_{BET} normalised (m^2 g^{-1})
		Fe_2O_3 (wt%)	Al_2O_3 (wt%)	Cr_2O_3 (wt%)	Fe (wt%)	Al (wt%)	Cr (wt%)			
–	10	87.4	17.4	0.0	86.1	13.0	0.01	58.9 ± 0.7	0.87	67.4 ± 0.8
0.001	30	88.7	22.7	0.6	85.2	16.5	0.56	72.9 ± 0.3	0.84	87.2 ± 0.4
0.0025	30	86.7	21.9	1.3	84.9	16.2	1.24	82.6 ± 0.4	0.84	98.5 ± 0.5
0.005	50	86.4	19.6	2.2	82.4	14.1	2.06	78.3 ± 0.3	0.86	91.5 ± 0.4
0.010	30	82.8	27.3	2.3	77.6	19.4	2.10	73.4 ± 0.3	0.79	93.0 ± 0.4
0.015	30	79.6	31.4	2.9	74.4	22.2	2.62	75.6 ± 0.4	0.75	101.2 ± 0.5
0.05	30	79.1	30.5	3.2	74.1	21.6	2.93	77.9 ± 0.4	0.75	103.4 ± 0.5

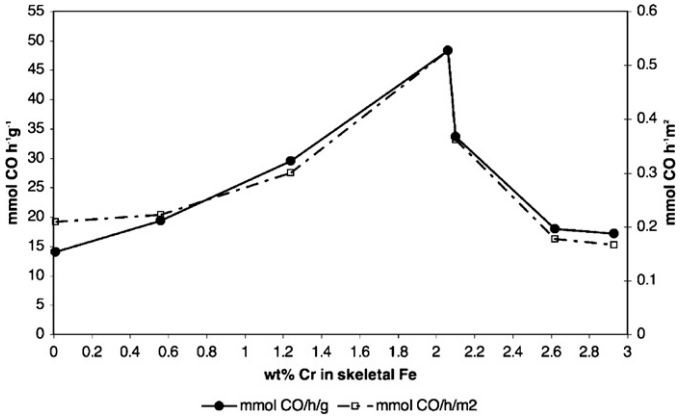

Fig. 4. Rates of conversion of CO per gram catalyst and per normalised m^2 for the WGS reaction versus wt% Cr in skeletal iron. Reaction conditions: gas flow = 50 ml CO/min and 50 ml Ar/min, rate of H_2O addition: 37 μl/min, operating temperature = 350 °C, pressure = 1 atm.

obtained from leaching in 3 M NaOH solutions containing sodium chromate contained a range of chromate compounds, including CrO, CrO_3, Cr_3O_8 and CrO(OH). For materials obtained from exposure to 0.005 M Na_2CrO_4 at 30 °C the chromium was incorporated with FeO as a chromite spinel ($FeO{\cdot}Cr_2O_3$). This observation may be indicative of a topochemical reaction, where the chromate species is introduced into the host of iron and iron oxides, which form during the leaching process. XRD patterns changed significantly with increasing chromate in alkali, which showed that the chromate indeed plays a role during the leaching reaction.

3.6. Catalyst activity for water–gas-shift

Table 6 shows the properties of the catalysts that were tested for the high-temperature WGS reaction. Fig. 4 shows the effect of chromium on the rate of CO conversion both on the basis of catalyst mass and BET surface area. The skeletal iron produced by leaching Fe_2Al_5 in a caustic solution of 3 M containing 0.005 M Na_2CrO_4 improved the conversion of carbon monoxide by a factor of 3.4 compared with the unpromoted skeletal iron catalyst. The results of this preliminary study of chromium promoted skeletal iron for the high-temperature WGS reaction in Fig. 4 are extremely interesting. They show that catalysts produced by the Raney method are indeed active for the WGS reaction. Furthermore, they show that the Cr (present as Cr_2O_3) has a marked effect on the activity of skeletal iron for the WGS reaction. This observation is contrary to the literature on chromia promoted porous iron WGS catalysts produced by other methods. The comprehensive reviews by Ratnasamy and Wagner [12] and Newsome [14] report that chromia acts solely as a catalyst stabiliser and not as a promoter.

In order to compare the activities of the Cr promoted skeletal iron of this study (Fig. 4) with the activity of a commercial iron oxide–chromium oxide catalyst we have used data from a paper by Bohlbro [22] who made extensive studies of the high-temperature WGS reaction. At atmospheric pressure and using almost identical feed compositions to that of this study he found reaction rates of 10.9 mmol CO h^{-1} g^{-1} at 330 °C and 42.0 mmol CO h^{-1} g^{-1} at 380 °C. Interpolating to 350 °C gave a value of 19.2 mmol CO h^{-1} g^{-1}. The results in Fig. 4 show that the Cr promoted catalysts of this study have slightly higher activities.

4. Conclusions

This study has shown that small additions of sodium chromate to 3 M NaOH used to leach particles of Fe_2Al_5 alloy led to decreased rates of leaching and changes to the morphology of the skeletal iron that is produced. This results from a slowing of the rate of Al dissolution from the Fe_2Al_5 particles. A preliminary investigation of the use of the chromia promoted skeletal iron catalysts shows that chromia acts as a significant promoter of iron when catalysing the high-temperature water–gas-shift reaction.

Acknowledgements

We express our thanks to Dr. Jason Scott for his guidance and advice on the water–gas-shift apparatus. The financial support of the Australian Research Council to the ARC Center of Excellence for Functional Nanomaterials for this research project is gratefully acknowledged.

References

[1] M. Raney, U.P. Office, 1,563,587, 1925.
[2] M. Raney, U.P. Office, 1,628,190, 1927.
[3] M. Raney, U.P. Office, 1,915,473, 1933.
[4] M. Raney, Ind. Eng. Chem. 32 (1940) 1199.
[5] R. Paul, G. Hilly, Bull. Soc. Chim. 6 (1939) 218.
[6] T.M. Leoni, PhD, Preparation and characterisation of skeletal iron catalysts, University of New South Wales, Sydney, 2010.
[7] T.M. Leoni, M.S. Wainwright, Curr. Top. Catal. 9 (2010) 41.
[8] Y.H. Zhou, M. Harmelin, J. Bigot, Mater. Sci. Eng. A 133 (1991) 775.
[9] Y.-J. Lü, Z.-X. Zhang, J.-L. Zhou, J. Nat. Gas Chem. 8 (1999) 82.
[10] Y. Lu, P. Zhou, W. Dongguang, Characterization of skeleton iron catalyst for slurry phase FT synthesis, in: Eighteenth Annual International Pittsburgh Coal Conference, Newcastle, Australia, 2001.
[11] P. Zhou, L. Abrams, C.M. Long, L. Yijun, U.P. Office, 6,903,141, 2005.
[12] C. Ratnasamy, J.P. Wagner, Catal. Rev. 51 (2009) 325.
[13] J.C. Gonzalez, M.G. Gonzalez, M.A. Laborde, N. Moreno, Appl. Catal. 20 (1986) 3.
[14] D.S. Newsome, Catal. Rev. 21 (1980) 275.
[15] C. Rhodes, G.J. Hutchings, A.M. Ward, Catal. Today 23 (1995) 43.
[16] T.M. Leoni, A.J. Smith, M.S. Wainwright, Top. Catal. 53 (2010) 1166.
[17] L. Ma, A.J. Smith, T. Tran, M.S. Wainwright, Chem. Eng. Process. 40 (2001) 59.
[18] A.J. Smith, L.O. Garciano, T. Tran, M.S. Wainwright, Ind. Eng. Chem. Res. 47 (2008) 1409.
[19] A.J. Smith, L.O. Garciano, T. Tran, Ind. Eng. Chem. Res. 47 (2008) 2518.
[20] L. Ma, B. Gong, T. Tran, M.S. Wainwright, Catal. Today 63 (2000) 499.
[21] L. Ma, M.S. Wainwright, in: D.G. Morrell (Ed.), Catalysis of Organic Reactions, Marcel Dekker, New York, 2003.
[22] H. Bohlbro, Acta Chem. Scand. 15 (1961) 502.